Electron Localization in Liquid Acetonitrile

I. A. Shkrob* and M. C. Sauer, Jr.

Chemistry Division, Argonne National Laboratory, Argonne, Illinois 60439

Received: March 20, 2002; In Final Form: June 18, 2002

Time-resolved one- and two-pulse laser dc photoconductivity has been used to observe two kinds of reducing species, anion-1 and anion-2, in liquid acetonitrile. At 25 °C, the standard enthalpy of conversion from anion-1 to anion-2 is -44.3 ± 3.6 kJ/mol and the conversion time is ~3 ns. The high-temperature form, anion-1, absorbs in the IR and migrates >3.3 times faster than any other ion in acetonitrile. This rapid migration has a low activation energy of 3.2 kJ/mol (vs ~7.6 kJ/mol for other ions). Anion-1 rapidly transfers the electron to acceptors with high electron affinity, with rate constant up to 10^{11} M^{-1} s^{-1}. The low-temperature form, anion-2, absorbs in the visible and exhibits normal mobility and electron-transfer rates, ca. 1.5×10^{10} M^{-1} s^{-1}. It reacts, by proton transfer, with two hydrogen-bonded molecules of water and/or aliphatic alcohols. Laser photoexcitation of these two solvent anions in their respective absorption bands leads to the formation of CH_3 and CN^-. We present arguments indicating that anion-2 is a dimer radical anion of acetonitrile, whereas anion-1 is a multimer radical anion that may be regarded as a "solvated electron".

1. Introduction

"Solvated" or "trapped" electron is a convenient but inconsistent way of describing the excess electron in a dielectric medium: a lone quantum-mechanical particle that interacts with (many) electrons and nuclei of the medium by means of an empirical classical potential.[1−12] The crucial step here is the reduction of a many-electron problem to a single-electron one.[3] In practice, this means that the effect of the "solvated electron" on the electronic structure of the solvent molecules is either ignored or introduced *ex postulato*.[1,2]

Although there are many theoretical works on the "solvated/trapped electron",[3−12] these works differ only in how the one-electron potential is chosen. In recent models, more "realistic", time-dependent model potentials are used.[9−12] As for the justification of the one-electron approach that underlies these models, no progress has been made. Meanwhile, one-electron models popular in the 1960s have been abandoned, both in quantum chemistry and computational chemical physics, in favor of more rigorous approaches in which many-body effects (such as the electron correlation) are adequately represented.

The one-electron approach provides insight concerning many properties of the excess electrons in water and alcohols, in particular, their optical spectra and energetics,[3,6,8,9,11] diffusion,[12] solvation/relaxation dynamics,[5,9−12] etc. At the same time, this approach, however advanced, is incapable of accounting for many other properties of the excess electron.[4] For instance, the low *g*-factor of the "solvated electron" is indicative of Pauli exclusion of its wave function by the electrons in the solvent molecules. Naturally, Electron Paramagnetic Resonance (EPR) spectroscopists favor the models in which the "trapped electron" is treated as a multimer anion; this tendency is most strongly expressed in the publications of Kevan and co-workers.[4,7] For example, for "trapped electrons" in glassy alkanes, it proved impossible to construct a model classical potential (that would account for the EPR data) without postulating induced dipoles along stretched C−C bonds.[7] This stretching is due to sharing of the electron density by the alkane molecules; such sharing is impossible in the one-electron models. There are many other properties of the "solvated electron" that cannot be represented in the one-electron approximation, such as its Raman spectrum,[13a] proton-transfer reactions, temperature dependence of the spectra over wide range of physical conditions, etc. Currently, there is a renewed interest to the alternative, multimer anion, approach, as it naturally emerges in the studies of medium and large size cluster anions (such as $\{H_2O\}_n^-$) in the gas phase.[13b]

Apart from a few liquids for which the features of the "solvated electron" are explicit, the concept of the "solvated electron" is impractical. In most organic liquids, the electron is thought to attach, permanently or temporarily, to one or two solvent molecules ("monomer or dimer radical anions"); the negative charge is fully localized on these anions. Surprisingly, there is not much evidence that such anions occur in nonaromatic liquids. Another possibility is that the electron is attached to many solvent molecules at once, forming a multimer anion. The "solvated/trapped electron" is a variant of this multimer anion.[4] Though the notion of the "multimer anion" is vague, it is the only one available to describe solvent anions in many practically important liquids, such as C_6F_6[14a] and supercritical CO_2.[15,16] These liquids are the extreme examples of what happens in any dielectric medium: drastic adjustment of the electronic structure of the solvent in response to the excess negative charge.

In this respect, "organic water", acetonitrile, makes an interesting case in point. In the gas phase, CH_3CN, like water and aliphatic alcohols, has a large dipole moment and negative vertical electron affinity.[17] One would expect that the electron in acetonitrile localizes much in the same way as the "solvated electron" in water and alcohols. Although this is what was believed initially,[18] further studies showed a different picture:

There are at least two reducing species present in liquid acetonitrile shortly after the ionization event: anion-1 that absorbs in the 1−2 μm region (whose band is centered at 1.45 μm) and anion-2 that absorbs in the 400−800 nm region (whose

* To whom correspondence should be addressed: Tel: (630) 252-9516. Fax: (630) 252-4993. E-mail: shkrob@anl.gov.

10.1021/jp0207580 CCC: $22.00
Published on Web 08/30/2002

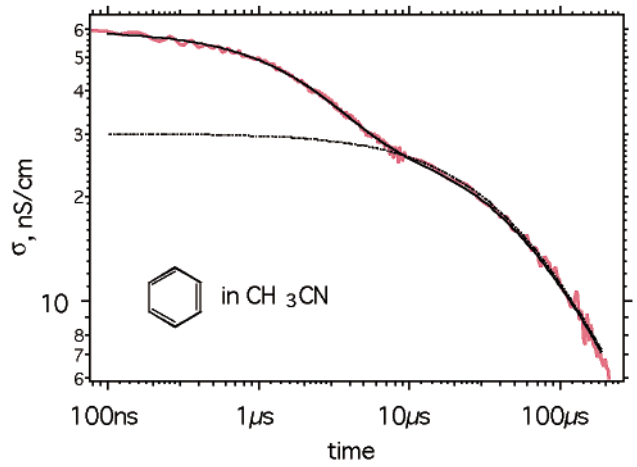

Figure 1. Typical dc photoconductivity kinetics $\sigma(t)$ *(dots)* obtained in biphotonic 248 nm ionization (15 ns fwhm, 0.03 J/cm^2) of 300 μM benzene in room-temperature argon-saturated acetonitrile (2 cm cell, 1.23 kV/cm). The fast conductivity signal with lifetime of 2.7 μs is from high mobility solvent radical anion(s). The solid line is the least-squares fit obtained using eq 3; the dashed line is the contribution from the normally diffusing ions. In all figures, the conductivity is given in nanoSiemens per centimeter (1 nS/cm = 10^{-7} Ω^{-1} m^{-1}).

band is centered at ~500 nm).[19] These two anions are in a rapid dynamic equilibrium: as the liquid is cooled, the 1.45 μm band becomes more and the 500 nm band less prominent. From the temperature dependencies of the transient absorption spectra, Bell, Rogers, and Burrows (in the following, referred to as BRB) estimated that anion-2 is 0.36 eV more stable than anion-1.[19] The transformation of anion-1 to anion-2 is rapid at room temperature but fairly slow at lower temperatures; at −30 °C, it takes at least 20−50 ns. BRB suggested that anion-1 and anion-2 are, respectively, the monomer and the dimer radical anions of acetonitrile. Below, their arguments will be considered in more detail.

In the present work, time-resolved laser photoconductivity was used to demonstrate several new features of these two solvent anions. It is shown that (i) while anion-2 has normal mobility, anion-1 is a high-mobility species whose room-temperature diffusion coefficient is more than three times higher than that of other ions, (ii) the activation energy for this migration is ~3.2 kJ/mol, whereas that of normal ions (including anion-2) is ~7.6 kJ/mol, (iii) electron-transfer reactions that involve anion-1 proceed with rate constants approaching 10^{11} M^{-1} s^{-1}, (iv) proton-transfer reactions of anion-2 involve two solute molecules and proceed 10 to 10^3 times slower than the rapid electron-transfer reactions, and (v) photoexcitation of anion-1 and anion-2 in their respective bands causes their fragmentation.

Using these dc conductivity data, EPR data of Williams and co-workers[20−22] for radical anions in solid nitriles, pulse radiolysis results of refs 19 and 23, and density function calculations for $\{CH_3CN\}_n^-$ clusters in ref 24 and in this work, we argue that anion-2 is a planar side-by-side $\{CH_3CN\}_2^-$ dimer anion, whereas anion-1 is a multimer anion related to the "trapped electron" in frozen glassy alkanes. To save space, many pieces of data are given in the Supporting Information. Figures, tables, and sections with a designator "S" after the number (e.g., Figure 1S) are placed therein.

2. Background

We first consider the data on acetonitrile cluster anions in the gas phase, then EPR and optical spectroscopy of $\{CH_3CN\}_n^-$ anions (n = 1, 2) in solid acetonitrile, and end with a brief summary of pulse radiolysis, laser photolysis, and photoconductivity studies of liquid acetonitrile.

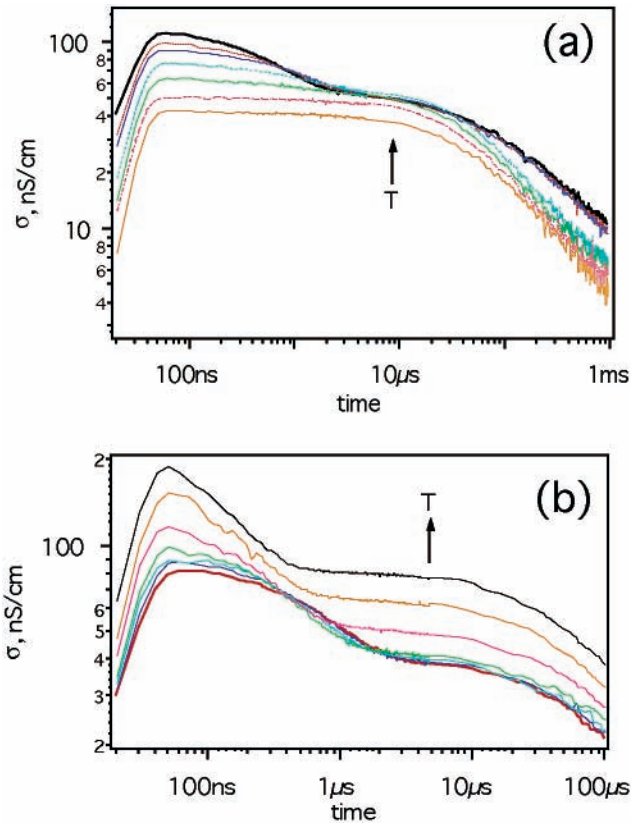

Figure 2. Temperature dependence of the conductivity kinetics obtained under excitation conditions similar to those shown in Figure 1. The decay constants of the fast conductivity signal are given in Figure 3(a). The sample temperatures were, from bottom to top: (a) −36, −26, −15, −5, +5, +12, +22 °C and (b) 21.7, 27.3, 33.7, 40.3, 44.9, 51.1, and 53.9 °C. As the temperature decreases, the fast conductivity signal decreases relative to the long-lived signal and its decay slows down. Note that the long-lived signal from normally diffusing ions increases with temperature several times faster than ion mobility (Figure 10S), suggesting a large temperature effect on the photoionization yield.

Gas-Phase Cluster Anions. In the gas phase, monomer CH_3CN has a dipole moment of 4.3 D, adiabatic electron affinity of 17 meV, and vertical electron affinity of −2.84 eV.[17] CH_3CN^- is a classical example of the dipole-bound anion postulated by Fermi and Teller, with the electron in a diffuse orbital (>30 Å). Although neutral dimers, in which the CH_3CN dipoles are coupled in the antiparallel fashion, readily form in vapor,[25,26] the dimer anion, $\{CH_3CN\}_2^-$, has never been observed. In the neutral trimer, one of the monomers couples sideways to the antiparallel pair; this molecule binds the electron in the same way as the monomer; the adiabatic electron affinity of this trimer (14−20 meV) is higher than that of the monomer.[17] Higher multimer anions, $\{CH_3CN\}_n^-$, prepared by collisional electron transfer from high-Rydberg atoms were found only for n > 12:[27] it takes many acetonitrile molecules to stabilize the negative charge. *The stabilization of the core "monomer" and "dimer" anions in solid and liquid acetonitrile is a concerted effect of many solvent molecules.*

Anions in Solid Acetonitrile. Solid acetonitrile exists in two crystalline forms, monoclinic α-acetonitrile and orthorombic β-acetonitrile (Figure 1S).[28,29] When these solids are γ-irradiated at 77 K, α-acetonitrile yields a dimer radical anion (Figure 2S), whereas β-acetonitrile yields a monomer radical anion (Figure 3S). The observed dichotomy follows from the crystal structure.

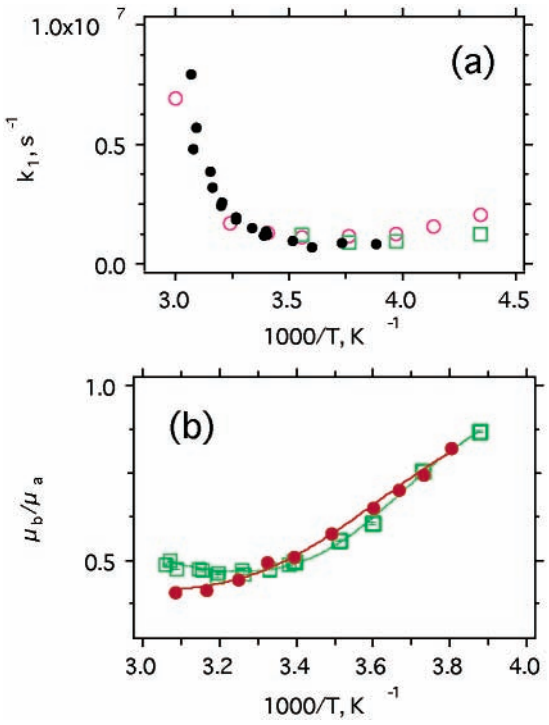

Figure 3. Temperature dependencies in Ar-saturated acetonitrile of the pseudo-first-order decay constant k_1 of the fast conductivity signal *(filled circles, traces (a))* and the ratio μ_b/μ_a of the mobilities for normally diffusing (impurity or solute) anion (b) and high-mobility solvent anion (a) *(traces (b)*. See the text for the details of the kinetic analysis. In traces *(a)*, the decay constants of 550 nm *(open squares)* and 1450 nm *(open circles)* transient absorbance from anion-2 and anion-1, respectively, are shown for comparison (from pulse radiolysis data of ref 19). As a function of temperature, the fast conductivity signal decays in the same way as these two anions, and the impurity limited lifetimes are similar. In traces (b), two sets of data are shown: for anion (b) being chloride *(filled circles)* and for anion (b) being an unidentified impurity anion *(open squares)*. The chloride data were fit using eq 5 with parameters given in section 4.2C. Both of these temperature dependencies are non-Arrhenius. This is due to a fast dynamic equilibrium between the high-mobility metastable anion-1 and low-mobility stable anion-2.

In α-acetonitrile, the dimer anion retains the same reflection plane and inversion center as the C_{2h} symmetric antiparallel pair of CH_3CN molecules (Figure 1S(a)).[20,24,28] β-Acetonitrile consists of infinite chains of parallel dipoles,[29] Figure 1S(b), and a monomer anion is formed instead.[24]

EPR experiments indicate that the dimer radical anion has a staggered, side-by-side structure shown in Figure 2S(a). The C−C−N angle is 130° and the distance between cyanide carbons is 1.65 Å. The negative charge and unpaired electron density are mainly on carbonyl N and methyl C atoms (Figure 2S(b)). This structure accounts for the observed EPR parameters and vibronic progressions observed in the 530 nm charge-resonance band.[20,24] The monomer radical anion in β-acetonitrile is also bent (Figure 3S(a)); the CCN angle is ∼131°. In both of these radical anions, the C−C bond is stretched to 1.53 Å (vs 1.443 Å in CH_3CN). Photoexcitation of these radical anions (λ < 650 nm) causes further elongation of the C−C bonds which leads to their fragmentation to CH_3 and CN^-.[20,24] Save for the vibronic progressions, both radical anions exhibit similar absorption spectra in the visible (see Figure 3 in ref 20). For the dimer radical anion, the band is centered at 530 nm, for the monomer radical anion, at 420 nm.[20] The positions of these bands are in good agreement with *ab initio* calculations.[24] These calculations indicate that no bound-to-bound transition in the IR is possible, either for the monomer or the dimer radical anion.[24]

Pulse Radiolysis and Photolytic Studies on Liquid Acetonitrile. Some results have already been discussed in the Introduction. At 25 °C, the interconversion of anion-1 and anion-2 is fast (<10 ns).[19,23] Consequently, in the presence of an electron acceptor, both species decay with the same rate constant. Even weak electron acceptors, such as N_2O, rapidly react with these anions.[19] For electron acceptors with high electron affinity, the scavenging constants are $(3-6) \times 10^{10}$ M^{-1} s^{-1},[19,35] which is considerably higher than the rate constant for ordinary diffusion controlled reactions in acetonitrile ($\sim(1-1.5) \times 10^{10}$ M^{-1} s^{-1}). Therefore, at least one of these solute anions has anomalously high mobility.

The same conclusion was supported by the photoconductivity studies of Hirata and et al.,[30] who examined monophotonic ionization of aromatic amines in room-temperature acetonitrile. Within 200 ns after the photoionization event, there was a strong conductivity signal from a radical anion; this species reacted with biphenyl and CCl_4 with approximately the same rate constants as the anions identified by BRB. Hirata et al.[30] suggest that (i) this conductivity signal is from anion-2 (the dimer anion) and (ii) submicrosecond decay of this species is due to further polymerization of the dimer anion. As shown below, the conductivity signal is actually from anion-1 and the short decay time is due to a reaction with impurity. Using picosecond pump−probe laser spectroscopy, Hirata et al. found that the 500−700 nm band of anion-2 was present as early as 1−3 ns after a 30 ps excitation pulse.[35]

The identification of anion-1 as the monomer and anion-2 as the dimer anion suggested by BRB[19] and others[23,30] is conjectural. In solid acetonitrile, both anions absorb in the visible;[20] there are no NIR bands. Furthermore, it is unprecedented that a monomer ion absorbs to the red of the dimer ion. The 1.45 μm band of anion-1 looks much like the absorption band of the "solvated electron" in liquid and vitreous alkanes.[1,2,4,7] BRB suggested two reasons, why anion-1 is a monomer anion rather than, say, such a "solvated electron":[19]

(a) First, it was found that anion-1 decays in reactions with water and alcohols, by proton transfer ($n = 1$)

$$\{CH_3CN\}_n^- + ROH \rightarrow (n-1)CH_3CN + CH_3(H)C{=}N^{\bullet} + RO^- \quad (1)$$

Using EPR spectroscopy, Chandra and Symons observed and characterized the resulting H-adduct radical, $CH_3(H)C{=}N^{\bullet}$, in γ-radiolysis of CH_3CN in CD_3OH glass at 77 K.[31] The absence of the corresponding D-atom adduct in the EPR spectra obtained from the CD_3OH glass suggests that proton-transfer reaction 1 involves hydroxyl protons of methanol, in agreement with pulse radiolysis studies of Meisel and co-workers.[23]

According to BRB,[19] the occurrence of reaction 1 proves that anion-1 is not a "solvated electron" because the latter species do not react with water and alcohols. This argument is dubious: in aliphatic alcohols, "solvated electrons", both in their ground state and in their excited state, abstract a proton from the solvent, in 1−10 μs[32] and 1 ps,[33] respectively. Furthermore, because anion-1 and anion-2 are in rapid equilibrium, it is not obvious, which one of these anions actually reacts. In the subsequent study by Meisel and co-workers,[23] the VIS absorbance from anion-2 was shown to decay, upon addition of alcohols, in the same way as the NIR absorbance from anion-1. From the temperature dependence of these kinetics, it was concluded that the reacting species is anion-2. Though the actual reaction mechanism is more complex than that considered by

either group (section 2S), our conductivity study supports the latter conclusion.

(b) The second argument[19] was that in radiolyzed toluene and THF solutions containing more than 5 vol % of CH_3CN, the NIR absorbance (of anion-1) was the same as that in neat acetonitrile.

Dimer radical cations of toluene strongly absorb in the NIR and contribute prominently to the spectrum of radiolysed toluene;[34] "solvated electrons" in THF also absorb in this region.[2] Thus, more than one absorbing species was present in the radiolysate. Even if there were no dimer cation absorbances and the electrons were irreversibly attached to acetonitrile, in the specified concentration range (5−20 vol %), acetonitrile is known to agglomerate forming pentamers and heptamers (section 3S).[35,36] It is conceivable that acetonitrile multimers solvate the electron in a similar way as neat acetonitrile. In alkanes, alcohol tetramers[37] readily trap the electrons;[38] the resulting $\{ROH\}_4^-$ multimer anions exhibit nearly the same optical and EPR spectra as the "solvated electrons" in neat alcohols. *The concentration of acetonitrile in the experiments of BRB was too high, and it is not clear that monomer anions were formed under such conditions.* Furthermore, it is doubtful that such monomers could form at all in the mixtures: Williams and co-workers have studied γ-irradiated acetonitrile-MTHF solutions at 77 K (5 to 40 vol %) and found no evidence for the formation of CH_3CN^- (with EPR spectrum of the monomer radical anion in β-acetonitrile) or $\{CH_3CN\}_2^-$ therein.[21]

Nevertheless, the basic reasoning is sound: in a sufficiently dilute solution, acetonitrile must be present as a monomer. Provided that this monomer scavenges the electron, a "monomer anion" would form. The properties of this monomer anion could be compared to those for anion-1 in neat acetonitrile. This program is implemented below.

3. Experimental Section

Temperature dependencies of density, viscosity, and ion mobilities in acetonitrile were taken from ref 39. Biotech grade acetonitrile-h_3 (99.93+%) stored under nitrogen was obtained from Aldrich and was used without purification, but without exposure to air. This solvent exhibited the same or longer lifetimes for anion-1 as purified solvent used in previous pulse radiolysis studies.[19,23] In acetonitrile-d_3 (99.6 at. % D acetonitrile-d_3 from Aldrich), the lifetime of anion-1 was 5−10 times shorter than in acetonitrile-h_3, due to scavenging by impurity. Spectrophotometric grade *n*-hexane (95+%, Aldrich) was purified by passage through a column of activated silica gel. Deuterated and protiated alcohols and electron acceptors were obtained from Aldrich and used as received.

Acetonitrile solutions were purged with argon and contained in a glass-ceramic conductivity cell with a 1 cm optical path, an internal volume of 4 cm^3, and a cell factor of 2.46 cm^{-1}. The distance between Pt electrodes was 6.5 mm. The conductivity cell was operated at 300−2000 V. At 25 °C, the voltage was typically 800 V; at lower temperatures, it may be increased to a few kV. When the cell filled with acetonitrile is first exposed to the high voltage, there is a spike of dark current that, over a period of time, reduces to 10−30 μA and then stabilizes. This dark current is due to traces of an electrolyte (such as acetic acid) in the solvent. Short exposure of the solution to 1−3 kV further reduces the dark current. Because this current does not change upon photoexcitation, it may be numerically subtracted from the conductivity traces (< 1 ms). The photocurrent through 50 Ω was amplified 100−1000 times and acquired using a DSA-601 digitizer; the response time of the detection system was 2−3 ns.

The conductivity cell was placed in an aluminum jacket; cold hexane (down to −30 °C) was circulated through the jacket using an FMS Systems model MC880A1 cryogenic bath. Above room temperature (up to 50 °C), hot water was circulated. Alternatively, we used an RTE−140 bath filled with a water−ethylene glycol solution (−40 and 60 °C).

The solutes were ionized using a 248 nm (5 eV) photon pulse from a Lambda Physik LPX 120i KrF excimer laser (15 ns fwhm, <100 mJ). Typically, the light fluence of the collimated UV beam through a 4 × 6 mm aperture was 0.02−0.05 J/cm^2. In most experiments, 300 μM benzene was used as a photosensitizer (section 4.2). The decay kinetics of the conductivity did not change with the benzene concentration. The dependence of the maximum conductivity signal σ on the 248 nm laser fluence indicates that the ionization of benzene (and naphthalene) is biphotonic (the photon orders are 1.91 ± 0.02 and 1.78 ± 0.07, respectively). For aromatic hydrocarbons with lower ionization potential, the ionization is monophotonic. For perylene, the photon order is 1.52 ± 0.11 (2 × 3.57 eV photon ionization of pyrene and perylene has been reported in ref 40), for triphenylene—1.08 ± 0.09; for anthracene—1.1 ± 0.3. Monophotonic ionization of aromatic amines (upon 3.5−3.6 eV photoexcitation)[30,40] and anthracene (upon 5 eV photoexcitation)[41] in acetonitrile have been reported previously. Neat acetonitrile also yields a conductivity signal. Under the same excitation conditions, this signal is 150−200 times smaller than that from the 300 μM benzene solution. The low photon order of this signal (1.67 ± 0.08) suggests an ionizable aromatic impurity.

In some experiments, the solute was ionized using 248 nm laser pulse and the anion(s) were subsequently photoexcited using a second laser pulse of a different color. A Continuum model 8010 Nd:YAG laser was used to generate 1064 nm (<0.6 J/cm^2) or 532 nm (second harmonic, <0.3 J/cm^2), 8.6 ns fwhm pulses. The two laser beams were coaxial and traveled in opposite directions. The beam from the Nd:YAG laser was passed through a 4 mm diameter aperture; within the cell, this beam enveloped the 248 nm beam which was passed through a 3 mm diameter aperture. Typically, the delay time of the second laser pulse was 150 ns. The laser fluences J_p given below are the *average* fluences through the apertures measured using a Gentec EM-1 meter with an ED-500 sensor. The kinetics with (σ_{on}) and without (σ_{off}) the second excitation pulse were collected on alternative 248 nm laser pulses and subtracted numerically. Typically, 16−32 kinetics were averaged in this way.

4. Results

4.1. "Monomer Anion" of Acetonitrile in *n*-Hexane Solution. To save space, the experimental details of the studies on negative charge dynamics in *n*-hexane solutions of acetonitrile are given in section 1S and Figures 1S−9S in the Supporting Information. Following the strategy outlined in section 2, we sought to establish the optical properties and energetics of CH_3CN^- anion in an inert matrix. If this matrix-isolated species existed and had similar properties to anion-1 observed in liquid acetonitrile, this (following the argument of BRB) would strongly support the identity of anion-1 as a metastable CH_3CN^- anion.

It was found that in dilute *n*-hexane solutions (< 1 vol % of CH_3CN), the electron reversibly attaches to acetonitrile monomer forming a slowly migrating negative charge carrier that can be formally regarded as a CH_3CN^- anion. Photoexcitation of the resulting anion with 532 and 1064 nm light results in electron detachment to the solvent that is followed by rapid reestablishment of the equilibrium between the CH_3CN^- anion

and the thermalized electron. Transient absorption spectroscopy of pulse-radiolyzed *n*-hexane solutions showed that CH_3CN^- has a NIR spectrum that is similar to that of the "solvated electron" in neat *n*-hexane; this spectrum does not resemble at all the spectrum of anion-1 in neat acetonitrile.

It appears that CH_3CN^- in *n*-hexane absorbs light via a bound-to-continuum transition from a shallow electron trap. Such a conclusion is supported by the energetics: CH_3CN^- is ~0.2 eV lower in energy than the "solvated electron" (section 1S) whose energy, in turn, is 0.6−0.8 eV lower than the energy of the conduction band electron.[42] Hence, a 1.17 eV (1064 nm) photon would suffice to promote the electron from CH_3CN^- directly to the conduction band of the solvent. These energetics rule out a molecular anion as a product of the electron attachment to CH_3CN. Since the lifetime of "CH_3CN^-" is >2 ns (section 1S), this must be a fully solvated species. Density functional calculations (B3LYP/6-31+G** method[43] in the IEF polarized continuum model of Tomasi et al.[44]) suggest that the free energy of solvation of CH_3CN and fully relaxed CH_3CN^- in *n*-hexane are 50 meV and 1.16 eV, respectively (for CH_3CN^-, the structure determined for the monomer anion in β-acetonitrile was assumed).[20,24] The energy of thermalized electron in *n*-hexane is −(0−0.1) eV[45,46] and the gas-phase adiabatic electron affinity of CH_3CN is ~17 meV.[17] Therefore, if CH_3CN^- were the product of electron attachment, the heat of this reaction would be at least −1 eV. This estimate compares favorably with the heats of electron attachment to other "shallow" traps: oxygen (~−2 eV),[47] CO_2 (~−1 eV),[48] pyrimidine (~−0.86 eV),[49] benzene,[45] and N_2O[50] (ca. −0.5 eV for both). For all of these species, the electron attachment causes large decrease in the entropy due to ordering of the solvent around the molecular anion:[46] e.g., for CO_2, the reaction entropy is −(50−60) J/mol·K,[48] for benzene ~−130 J/mol·K,[45] for other aromatic hydrocarbons, it varies between −80 and −200 J/mol·K.[46] By contrast, the standard entropy of electron attachment to CH_3CN is −15.4 J/mol·K (section 1S).

The standard heat of electron attachment to CH_3CN is extremely small, −19.6 ± 0.94 kJ/cm (section 1S). Such low binding energies have previously been observed only for the electrons trapped by alcohol dimers, RO(H)..HOR.[16,37] The resulting anion is a variant of the "solvated electron" that includes two hydrogen-bonded solute molecules in addition to several solvent molecules; the absorption spectrum of these "trapped" electrons is similar to that of the "solvated electron" itself. Apparently, a similar reaction occurs in *n*-hexane solutions of acetonitrile: electrostatic binding of the "solvated electron" to a single CH_3CN dipole is sufficiently strong to temporarily halt the electron migration. Because the dipole moment of CH_3CN is >2 times that of a typical alcohol (4.3 D for CH_3CN[17] vs 1.64−1.69 D for alcohol monomers in the gas phase),[51] just one CH_3CN molecule would bind the electron as readily as the alcohol dimer.

We conclude that "CH_3CN^-" in *n*-hexane is a "solvated electron" that is dipole bound to a single acetonitrile molecule. BRB argued[19] that anion-1 in neat acetonitrile must be a monomer radical anion because the reducing species in dilute solutions of CH_3CN absorbs such as this anion. This similarity was not observed in our study. Furthermore, BRB presumed that the reducing species in these dilute solutions is a molecular anion. This assumption is also incorrect, and the whole argument is invalid. Anion-1 is unique to liquid acetonitrile; no such species or its analogues are formed in dilute solutions.

4.2. Conductivity Kinetics in Liquid Acetonitrile. Typical dc conductivity traces observed in biphotonic 248 nm ionization of benzene in liquid CH_3CN are shown in Figure 1. As in other polar liquids, no geminate recombination was observed on the time scale of our conductivity experiment; these kinetics must be over in less than 1 ns. In the first few microseconds after a 15 ns fwhm 248 nm excitation pulse, the conductivity signal $\sigma(t)$ exhibits fast exponential component (Figures 1 and 2) whose lifetime (k_1^{-1}) behaves, as a function of temperature, the same way as the lifetime of anion-1 in pulse radiolysis experiments of BRB (Figure 3(a)).[19] At 25 °C, the lifetime of this signal is 1−3 μs (depending on the particular batch) which is considerably longer than 200 ns observed in the conductivity experiments of Hirata et al.[30] The fast conductivity signal is removed upon the addition of electron-scavenging solutes, such as N_2O, CO_2, and CCl_4. The same fast signal was observed in photoionization of neat acetonitrile and several aromatic solutes other than benzene, including those that exhibited monophotonic and mixed-photon-order ionization (section 3). After the decay of this fast signal, there is a long-lived signal that decays over hundreds of microseconds (Figures 1 and 2). The decay of this signal follows second-order kinetics (dashed line in Figure 1) and is from stable ions. The corresponding decay time of ion recombination in the bulk is proportional to the initial ion yield, and the recombination constant is 50% lower than that given by the Debye equation for a liquid with a static dielectric constant $\epsilon \approx 36$ (at 25 °C), suggesting that ion recombination is not diffusion controlled.

In neat acetonitrile and in solutions with low concentration of aromatic solute (e.g., 5−20 μM anthracene or triphenylene), there is also a slowly growing conductivity signal that reaches maximum in 10−100 μs and then persists for ~1 s. This persistent signal apparently decays by discharge of the ions at the electrodes, indicating a mobility of 1.2×10^{-3} cm^2/Vs (comparable to that of Et_4N^+, Figure 10S).[39] Previously, similar slowly growing dc conductivity signals in acetonitrile were accounted for by ionization due to triplet−triplet annihilation;[52] perhaps the persistent ion observed in our experiments is from a triplet. No such signal is observed in the 150−300 μM benzene solutions that were used in our conductivity study.

For delay times $t > 30$ ns, the decay kinetics of the dc conductivity signal $\sigma(t)$ can be simulated using a model in which a short-lived ion (a) transforms, either spontaneously or in a reaction with impurity, to a less mobile ion (b). In our case, both of these ions are anions. Let C_a and C_b be the concentration of these two anions in mole/m^3, then the conductivity signal

$$\sigma = F(\mu_a C_a + \mu_b C_b) \tag{2}$$

where F is the Faraday constant, $\mu_a = \mu_a^- + \mu^+$ and $\mu_b = \mu_b^- + \mu^+$, where μ_a^- and μ_b^- are the mobilities of anion (a) and (b), respectively, and μ^+ is the mobility of the countercation. The decay kinetics of these anions are given by

$$dC_a/dt = -k_1 C_a - \chi \mu_a C_a C_+ \tag{3a}$$

$$dC_b/dt = +k_1 C_a - \chi \mu_b C_b C_+ \tag{3b}$$

where $C_+ = C_a + C_b$. At $t \rightarrow 0$, $C_a = C_0$ and $C_b = 0$. If the homogeneous neutralization of ions obeys the Debye−Langevin equation, the coefficient χ in eq 3 is $F/\epsilon\epsilon_0$, where ϵ_0 is the permittivity of vacuum and ϵ is the static dielectric constant of the solvent. Equation 3 was solved numerically, and the least-squares optimization of fitting parameters yielded $\sigma_0 = F\mu_a C_0$, the ion conductivity extrapolated to $t = 0$, the rate constant k_1 of the anion transformation, and the ratio μ_a/μ_b of the mobilities

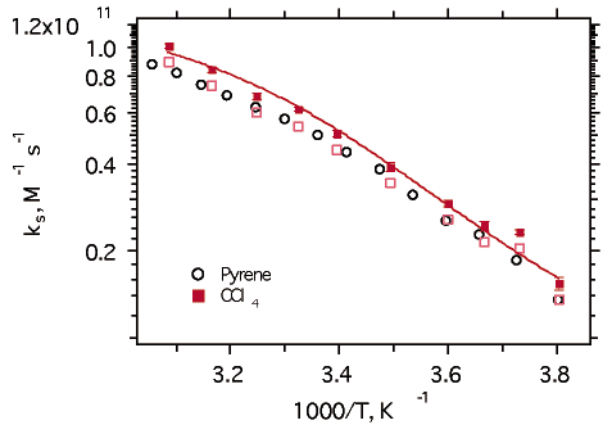

Figure 4. Temperature dependency in Ar-saturated acetonitrile of rate constants k_s for CCl_4 scavenging of the fast conductivity signal due to solvent anions plotted from the data of Figure 11S *(filled squares)*. Open squares indicate the same dependence scaled by 0.88. The temperature dependence for scavenging the 1450 nm absorbance from anion-1 by pyrene obtained in the pulse radiolysis experiment of BRB (ref 19) is shown for comparison *(open circles)*. It is clear that the two temperature dependencies are very similar. The solid line is the least-squares fit using eq 6 with kinetic parameters given in section 4.2C.

(these mobilities cannot be found separately, if χ is unknown). To measure these parameters with sufficient accuracy, the 248 nm laser power was attenuated so that the initial concentration of ions was ~1−50 nM and the second-order decay was at least 20 times slower than the decay of anion-1. Typical examples of simulated kinetics are given in Figures 1, 12S, and 13S.

Addition of CCl_4 causes disappearance of the fast signal. Figure 11S shows the concentration dependencies of the decay rate constants k_1 at several temperatures (−10 to 52 °C). All of these concentration dependencies are linear. We expect that CCl_4^- rapidly fragments yielding Cl^- whose mobility is known from conductometric studies (ref 39 and Figure 10S) and serves as a reference. At 25 °C, the rate constant k_s of scavenging the mobile anion (a) by CCl_4 is similar to that observed by BRB for anion-1.[19] Furthermore, k_s has a similar temperature dependence (Figure 4) to that observed for the rate constant of scavenging anion-1 by pyrene (the latter is ca. 22% lower, for all temperatures).[19]

As the temperature decreases, the decay of the fast conductivity signal slows down and the signal decreases in the magnitude (Figure 2). Below −15 °C, one cannot distinguish this signal at all. Figure 3(b) shows the temperature dependence of μ_b/μ_a for neat acetonitrile and CCl_4 solution. In the latter case, anion (b) is Cl^-. The non-Arrhenius behavior of this dependence suggests, in agreement with pulse radiolysis studies,[19,23] that at least two anions contribute to the fast conductivity signal. The observed behavior is consistent with a rapid dynamic equilibrium between a high-temperature (anion-1) and low-temperature (anion-2) solvent anions

$$\text{anion-1} \rightleftharpoons \text{anion-2} \tag{4}$$

provided that *anion-1* (rather than anion-2, as suggested by Hirata et al.)[30] is the high-mobility species. Let K_{eq} be the equilibrium constant of reaction 4. The mobility μ_a^- and the rate constant k_s of scavenging "anion (a)" defined in terms of eq 3 are given by equations

$$\mu_a^- = (\mu_1 + K_{eq}\mu_2)/(1 + K_{eq}) \tag{5}$$

$$k_s = (k_{1s} + K_{eq}k_{2s})/(1 + K_{eq}) \tag{6}$$

where k_{1s} and k_{2s} (μ_1 and μ_2) are the corresponding rate constants (mobilities) for the two solvent anions. If the temperature dependence of K_{eq} were known, one would be able to determine μ_{1s} and μ_{2s} (or k_{1s} and k_{2s}) separately. Although the equilibrium constant and its temperature dependence has been estimated by BRB,[19] those estimates were obtained with unproved assumption that the total yield of the solvent anions in radiolysis is independent of temperature. Furthermore, one needs more direct identification of the mobile species with anion-1. To this end, we studied photofragmentation of anion-1 and anion-2 by 1064 and 532 nm light, respectively.

A. 532 nm Photoexcitation of Anion-2. Upon the photoexcitation of the ionized acetonitrile solution with a 8.6 ns fwhm 532 nm pulse that is delayed within the duration of the fast conductivity signal, this signal decreases stepwise immediately after the excitation pulse (Figures 5(a), 12S, and 13S). The relative decrease in the fast signal does not depend on the delay time t_p of the 532 nm pulse (Figure 5(b)). With 0.25 J/cm^2 of 532 nm photons, it is possible to bleach 40−90% of the signal, depending on the temperature (Figures 14S and 15S). This bleaching can be interpreted in terms of photofragmentation of anion-2 that has an absorption band centered at 550 nm

$$\text{anion-2} + h\nu \rightarrow CH_3 + CN^- \tag{7}$$

This reaction is analogous to the reactions of monomer and dimer radical anions in solid α- and β-acetonitrile, respectively.[20] The resulting cyanide anion has approximately the same mobility as Cl^-. To include photofragmentation, the kinetic model considered above, which still applies at $t < t_p$, must be complemented with eq 8a, which accounts for the "instantaneous" change in the concentration of "anion (a)" at $t = t_p$

$$(1 - \Phi)C_a(t_p) \rightarrow C_a(t_p) \quad \textit{and} \quad \Phi C_a(t_p) \rightarrow C_c(t_p) \tag{8a}$$

where Φ is the conversion efficiency, and equations

$$dC_c/dt = -\chi\mu_c C_c C_+ \tag{8b}$$

$$\sigma = F(\mu_a C_a + \mu_b C_b + \mu_c C_c) \tag{8c}$$

that complement eq 3 for $t > t_p$; here C_c is the concentration of the cyanide anion, $C_+ = C_a + C_b + C_c$ is the cation concentration, and $\mu_c = \mu(CN^-) + \mu^+$. Because the mobility of CN^- is higher than that of the impurity anion ($\mu_c/\mu_b \sim 1.2$), there is a small net increase in the conductivity signal over the first 100 μs after the 532 nm pulse (Figures 5, 12S, and 13S). Experimentally, the kinetics with and without the 532 nm pulse (σ_{on} and σ_{off}, respectively) were obtained by blocking the 532 nm beam on alternative shots. The kinetic analyses were two-step: First, σ_{off} kinetics were fit to obtain k_1, χ, μ_a/μ_b, and σ_0, as described above. Then, these parameters were used to obtain the best estimates for Φ and μ_c/μ_b, by the least-squares fitting of $\sigma_{on} - \sigma_{off}$. Figures 5(b), 12S, and 13S show typical fits for σ_{off} and $\sigma_{on} - \sigma_{off}$ obtained by this procedure; the agreement is good, for all solvent temperatures.

The conversion efficiency Φ, determined by this analysis has been plotted vs the fluence of the 532 nm light, J_p, for several temperatures (Figures 14S and 15S). It is seen from this plot that the initial increase in Φ with the photon fluence is linear, i.e., reaction 7 is monophotonic. For a given photon fluence, the yield of photofragmentation systematically increases with temperature (Figure 15S; see also Figures 12S and 13S). This behavior is consistent with the occurrence of reaction 4: at lower

temperature, the equilibrium fraction of anion-2 increases and more species are bleached by the 532 nm light.

In the absence of equilibrium (4), the bleaching of anion-2 obeys the equation

$$\Phi = A\{1 - \exp(-BJ_p)\} \tag{9}$$

where $A = 1$ and $B = \sigma_2$ is the cross section of photo reaction. All the dependencies shown in Figure 15S may be fit using eq 9. Let τ_{eq} be the settling time of equilibrium (4), $J(t)$ be the time profile of a Gaussian laser pulse, $J(t) = J_p/\sqrt{\pi}t_{pulse}$ $\exp[-([t-t_p]/t_{pulse})^2]$, and C_0 be the sum of the concentrations of anion-1 and anion-2 before the 532 nm pulse. The equilibrium concentrations of anion-1 and anion-2 prior to the excitation are given by $C_{1,2}^0 = f_{1,2}C_0$, where $f_1 = 1/(1 + K_{eq})$ and $f_2 = K_{eq}/(1 + K_{eq})$ are their equilibrium fractions, respectively. During the laser pulse, these concentrations change according to

$$dC_1/dt = -\tau_{eq}^{-1}(f_2C_1 - f_1C_2) \tag{10a}$$

$$dC_2/dt = -\sigma_2 J(t)C_2 + \tau_{eq}^{-1}(f_2C_1 - f_1C_2) \tag{10b}$$

The fraction of the signal bleached is given by

$$\Phi = 1 - C_1(t{=}\infty)/C_1^0 = 1 - C_2(t{=}\infty)/C_2^0 \tag{11}$$

For a sufficiently small J_p

$$\beta = \partial\Phi/\partial J_p \approx f_2\sigma_2 \tag{12}$$

regardless of τ_{eq}. For arbitrary J_p, the analytical solution may be obtained only for $\tau_{eq} \gg t_{pulse}$ or $\tau_{eq} \ll t_{pulse}$. In both cases, eq 9 is still correct: For $\tau_{eq} \gg t_{pulse}$, $A = f_2$ and $B = \sigma_2$; for $\tau_{eq} \ll t_{pulse}$, $A = 1$ and $B = \beta$. In the general case, eq 10 has to be solved numerically, and Φ is a complex function of K_{eq}, τ_{eq}/t_{pulse} and σ_2. Experimentally (Figure 15S), A approaches unity only at low temperature. This suggests that at higher temperature, τ_{eq} and t_{pulse} are comparable. It is possible to estimate τ_{eq}, by numerical fitting of the fluence dependence $\Phi(J_p)$ using eqs 10 and 11, provided that the equilibrium constant K_{eq} is known. Figure 14S(b) shows how the optimum parameters σ_2 ($= \epsilon_2\phi_2$) and τ_{eq}/t_{pulse} determined by the least-squares fit of the fluence dependence in Figure 14S(a) depend on K_{eq}. From this point on, the cross section σ_2 is given as a product $\epsilon_2\phi_2$, where ϵ_2 is the decadic molar extinction coefficient of anion-2 at 532 nm, and ϕ_2 is the quantum yield of photo reaction 7.

To find the equilibrium constant K_{eq}, the fluence dependencies of Φ were fit using eq 9 and the product AB (which, according to eq 12, is equal to the initial slope β), was plotted as a function of the temperature, Figure 6(a). Because

$$K_{eq} = K_{eq}^0 \exp(-\Delta H_{eq}^0/R\{1/T - 1/T_0\}) \tag{13}$$

where K_{eq}^0 is the equilibrium constant and ΔH_{eq}^0 is the enthalpy of reaction 4 at $T_0 = 295$ K. Fitting the plot in Figure 6(a) yields $\sigma_2 = 1866 \pm 88$ M^{-1} cm^{-1} (assumed to be temperature-independent), $K_{eq}^0 = 1.32 \pm 0.2$, and $\Delta H_{eq}^0 = -44.3 \pm 3.6$ kJ/mol ($\sim$0.46 eV). The latter estimates are reasonably close to those obtained by BRB: $K_{eq}^0 = 0.6 \pm 0.1$ and $\Delta H_{eq}^0 = -38 \pm 2$ kJ/mol.[19] The agreement between the two sets of data indicate that the two-anion equilibrium model accounts both for the conductivity and pulse radiolysis data. Because our measurement is independent of the absolute ion yield, we believe it to be more accurate.

Using our estimate for K_{eq}^0 and the plot in Figure 14S(b), one obtains that at 23 °C, $\sigma_2 = 1887 \pm 70$ M^{-1} cm^{-1} (which is close to the estimate given above) and $\tau_{eq}/t_{pulse} = 0.5 \pm 0.06$. Using a fast photodiode, we determined $t_{pulse} = 6.2 \pm 0.2$ ns, so that $\tau_{eq} \approx 3.1$ ns. This short settling time justifies the use of eqs 5 and 6. BRB estimated that at -30 °C, $\tau_{eq} > 20-50$ ns.[19] The long settling time at the lower temperature suggests a considerable activation barrier for the transformation of anion-1 to anion-2.

According to BRB, the extinction coefficient of the 1450 nm band at 293 K (obtained with assumption that there is only one anion in the solution) is 23 000 M^{-1} cm^{-1}.[19] Because only anion-1 contributes to this IR band and the room-temperature equilibrium fraction of this anion is 43%, the extinction coefficient of anion-1 is 53 400 M^{-1} cm^{-1}. The absorbance at 532 nm is 14.5% of that at 1450 nm, whereas the equilibrium fraction of anion-2 is 57%. Therefore, the extinction coefficient of anion-2 at 532 nm is 5870 M^{-1} cm^{-1}, and the quantum yield of photofragmentation is 0.32.

In solid α- and β-acetonitrile, the net yield of the photofragmentation at 77 K strongly depends on the H/D substitution in the methyl group: most $\{CD_3CN\}_2^-$ pairs recombine, whereas $\{CH_3CN\}_2^-$ dissociate.[20] This behavior has been accounted for by a large quantum isotope effect on the mobility of methyl radicals in the crystalline lattice.[20] For anion-2 in liquid CD_3CN, the cross section of fragmentation is 9% lower than that for anion-2 in CH_3CN: the tunneling mechanism responsible for the large isotope effect in reaction 7 in frozen α- and β-acetonitrile[20] does not operate in the room-temperature liquid.

B. 1064 nm Photoexcitation of Anion-1. The 1064 nm photoexcitation causes the same photobleaching as the 532 nm photoexcitation (not shown). This indicates that either reaction 7 or an analogous reaction 14 for anion-1

$$\text{anion-1} + h\nu \rightarrow CH_3 + CN^- \tag{14}$$

takes place. The quantum efficiency of the 1064 nm photobleaching is low: the fluence dependencies are only slightly curved (Figure 16S). Even at high fluence ($\sim$0.6 J/cm^2), Φ is less than 0.5. The same procedure as in the previous section has been used to determine the initial slope β of Φ for several temperatures (Figure 6(b)).

When both anions are photoexcited, eq 12 must be replaced with

$$\beta \approx \sigma_1 f_1 + \sigma_2 f_2 \tag{15}$$

where σ_1 and σ_2 are the cross sections of reactions 8 and 14, respectively. According to eqs 13 and 15, β either increases or decreases with the temperature. The experimental β decreases with temperature below 20−25 °C; this may be expected if reaction 14 is the main photobleaching channel. However, it also decreases above 25 °C. The latter suggests that the 1064 nm cross sections of photo reactions 7 and 14 are temperature-dependent. Assuming the contrary, the low-temperature part of the curve in Figure 6(b) can be fit using eqs 13 and 15 for $\sigma_1 \approx 123 \pm 11$ M^{-1} cm^{-1} and $\sigma_2 \approx 14 \pm 4$ M^{-1} cm^{-1}. Although these estimates are approximate, it is clear that the species photobleached by the 1064 nm photons is mainly anion-1. Pulse radiolysis indicates that the 1064 nm absorbance of anion-1 is ca. 25% of its maximum absorbance at 1450 nm. This gives an extinction coefficient $\sim$13 400 M^{-1} cm^{-1} and a quantum yield of photofragmentation $\sim 10^{-2}$.

We conclude that both anion-1 and anion-2 fragment upon the photoexcitation in their respective bands.

C. Mobility and Electron-Transfer Reactions of Anion-1. Substituting the values obtained for the equilibrium parameters in eqs 5, 6, and 13, the mobility and rate constants for anion-1 and anion-2 can be estimated from the data shown in Figures 3(b) and 4. Note, that only a lower limit for μ_1 may be found from our data: anion-1 and anion-2 may not be the only anions initially present in the solution (as assumed in the data analysis). In particular, some solvent anions could be fragmented by the 248 nm light during the laser pulse. Furthermore, EPR studies on frozen nitriles (section 4S) suggest that dissociative charge transfer with the formation of alkyl radical and CN^- is the predominant mechanism for ionization of aromatic molecules in *solid* alkyl nitriles; to some degree this reaction may also occur in liquid acetonitrile. The only experimental result arguing against such a possibility is the fact that the relative magnitude of the fast signal (referenced to the long-lived signal from the impurity or solute ions) does not vary for different aromatic solutes, despite the variations in the ionization energetics and the photon order (section 3).

Assuming Arrhenius dependence for anion mobilities, we obtain $\mu_1 \approx 3.3 \times 10^{-3}$ cm^2/Vs at 25 °C and an activation energy for migration of anion-1 of 3.2 ± 0.5 kJ/mol. In this analysis, it was assumed that $\mu_2 \approx \mu^+ \approx \mu(Cl^-)$; for chloride, a mobility of 1.05×10^{-3} cm^2/Vs at 25 °C and an activation energy of 7.6 ± 0.1 kJ/mol were assumed from the conductometric data of ref 39 (Figure 10S). Assuming that scavenging reaction of solvent anions by CCl_4 is diffusion controlled (i.e., the activation energies for the corresponding reactions are the same as those for the anion diffusion), we estimate that at 25 °C, $k_{1s} = (1.03 \pm 0.03) \times 10^{11}$ M^{-1} s^{-1} and $k_{2s} = (1.46 \pm 0.3) \times 10^{10}$ M^{-1} s^{-1}. The rate constant for anion-2 is close to a typical rate of diffusion-controlled reaction in acetonitrile. The rate constant for anion-1 is indicative of a scavenging radius of 16.5 Å. Perhaps, the mobility of anion-1 is somewhat higher than 3.3×10^{-3} cm^2/Vs, because this reaction radius seems unreasonably large.

D. Reactions of Solvent Anions with Water and Alcohols. Proton-transfer reactions of solvent anions in acetonitrile with water and alcohols (reaction) have been studied by BRB[19] and by Meisel and co-workers.[23] It was noted by both groups that the concentration plots of the pseudo first-order constants k_1 were nonlinear (e.g., Figure 3 in ref 19), but no explanation for this nonlinearity was given. We have reinvestigated these reactions using time-resolved photoconductivity. Our results indicate that the proton-transfer reaction involves *at least two hydrogen-bonded ROH molecules*. Figures 17S to 21S and section 2S in the Supporting Information give the details of these photoconductivity studies and the proposed reaction mechanism. Though this reaction mechanism is more involved than was assumed in the previous studies, the improved kinetic analyses still support the main assertion of Meisel and co-workers:[23] the species involved in the proton transfer is anion-2 rather than anion-1. Thus, both arguments of BRB in favor of monomer radical anion as anion-1 (section 2) are shown to be incorrect.

5. Discussion

5.1. Synopsis of the Results for Neat Acetonitrile. The results of pulse radiolysis and laser photolysis of liquid CH_3CN are consistently explained in terms of two solvent radical anions, anion-1 and anion-2, in rapid dynamic equilibrium, reaction 4. At 25 °C, the settling time of this equilibrium is ~3 ns, the equilibrium constant is ~1.3, and the enthalpy of reaction 4 is −0.46 eV. The high temperature form, anion-1, absorbs mainly in the IR and migrates rapidly (>3.3 times faster than other ions at 25 °C) over a low potential barrier (~3.2 kJ/mol). In exothermic charge-transfer reactions, anion-1 is scavenged with a rate constant approaching 10^{11} M^{-1} s^{-1}. The low temperature form, anion-2, absorbs mainly in the visible, migrates normally, and reacts, also by charge transfer, with rate constants typical of other diffusion-controlled reactions in acetonitrile. This behavior suggests that anion-2 is a normal molecular radical anion. Unlike anion-1, anion-2 reacts with protic solutes, such as water and aliphatic alcohols, by hydroxyl proton transfer. The latter involves two solute molecules and proceeds either via a reaction of anion-2 with a solute dimer or via a two-step reaction mediated by the formation of unstable complex of anion-2 with the monomer solute (section 2S). Photoexcitation of anion-1 and anion-2 in their absorption bands causes their fragmentation to CH_3 and CN^-; there is no isotope effect for this photofragmentation.

5.2. Nature of Anion-1 and Anion-2. The formation of CH_3CN^- in solid β-acetonitrile is due to its favorable crystal structure. The only other nitrile in which a similar monomer was observed is the low-temperature form of crystalline NC-$(CH_2)_4$CN.[22] According to X-ray diffraction[35] and NMR[53] data, the short-range structure of liquid acetonitrile is similar to that of crystalline α-acetonitrile,[28] with a pentamer as the basic unit. The prevalent orientation of the acetonitrile molecules in the liquid is the antiparallel pair of the type found in α-acetonitrile; a linear head-to-toe arrangement is also possible. Given that dimerization strongly reduces the energy,[24] it seems likely that the monomer anion cannot form in liquid acetonitrile, where no "special arrangement" of neighboring molecules needed for the formation of the monomer anion is possible.

The evidence linking anion-2 to the dimer radical anion observed in solid α-acetonitrile is indirect. As discussed in section 2, the absorption spectrum of the monomer anion in β-acetonitrile is similar to that of the dimer anion in α-acetonitrile,[20] save for the red shift in the latter. The 550 nm absorption band of anion-2[19,23] is consistent with the dimer anion; fragmentation of anion-2 to CH_3 and CN^- upon the 532 nm excitation is also consistent with the low-temperature EPR data.[20] Furthermore, since anion-2 prevails in the cold liquid, it is likely to prevail in the high-temperature crystal (α-acetonitrile) which has very similar molecular structure to the liquid.[28,35] By contrast, β-acetonitrile (which yields monomer anions) has molecular packing entirely different from that of the liquid.[29,35]

In our view, the decisive argument in favor of identification of anion-2 as the dimer radical anion comes from the observation that anion-2 is a long-lived molecular anion in the lowest-energy form with normal migration and reaction properties. *Ab initio* calculations of ref 24 identify the dimer anion shown in Figure 2S(a) as the most stable acetonitrile anion. Strong two-center-three-electron bonding between the cyanide carbons accounts for this stability; such a stabilization mechanism is lacking in the monomer anion. For the latter species to be lowest-energy, the neighboring acetonitrile molecules should all be oriented in the same direction, as in β-acetonitrile; otherwise, coupling to a neighboring (antiparallel) molecule reduces the overall energy. It is difficult to see how such a fortuitous orientation could persist for ~3 ns in a room-temperature liquid.

Could a monomer anion account for the observed properties of anion-1? We have already considered the arguments of BRB[19] in favor of such an identification (section 2). The first of these arguments was refuted by Meisel and co-workers[23] and by results of this work (section 2S). The second argument was also refuted: in dilute acetonitrile solutions, CH_3CN^- does not form

and the IR spectra of "trapped electrons" in these solutions are different from those of anion-1.

We cannot offer better arguments. The monomer anion does not account for the absorption spectrum of anion-1. The relative stability of anion-1 in the liquid is an aspect for which it is impossible to account. Finally, it is not clear why a monomer anion would migrate rapidly. The only fast migration mechanism possible for the monomer anion would be charge hopping. Assuming that this hopping is between neighboring molecules (separated by 3.8−4 Å) and a diffusion coefficient is 8.3×10^{-4} cm^2/s (estimated from the room-temperature mobility of 3.3×10^{-4} cm^2/Vs), the residence time τ_h for the charge on a given molecule is ∼2 ps. This implies that $\sim 10^3$ hops occur prior to the transformation of the monomer anion-1 to anion-2. The lowest bending modes of the CCN fragment of acetonitrile molecules and anions are 300−330 cm^{-1} [24,54] which is equivalent to ∼0.1 ps in time units. Thus, though the diffusion is fast, the lifetime of a given "monomer anion" is sufficiently long for the structural relaxation; in other words, this "monomer anion" must be a bent species such as CH_3CN^- in β-acetonitrile.[20,24] Thus, the low-barrier resonant charge transfer needed to explain the high mobility would have to be between a strongly bent anion and a linear neutral molecule. Such a process cannot proceed with a low activation energy because bending of the neutral molecule and solvation of the resulting anion requires much energy. Furthermore, never once in a series of these 10^3 hops could the two molecules involved in the resonant charge transfer be in the antiparallel orientation, since then anion-1 would couple to the neighboring molecule yielding anion-2. It appears that the monomer anion cannot account for any property of anion-1.

Several previous examples of high-mobility anions have been reported in molecular fluids, by Warman and co-workers,[14a] in C_6F_6, by Itoh and Holroyd,[14b] in high-pressure benzene and toluene, and by Shkrob and Sauer,[15,16] in supercritical CO_2. In all of these cases, the activation energies for the migration of the solvent anions were relatively large: 11, 12−13, and 46 kJ/mol, respectively. Because the absorption[14a] (or electron photodetachment)[15] spectra were different from those of the corresponding monomer anions in dilute solutions Warman and co-workers[14a] and Shkrob and Sauer[15,16] suggested that these high-mobility species were multimer anions. The case of CO_2 is particularly illuminating because it also involves strong bending of the molecule upon electron attachment.[55] This bending requires considerable thermal activation, even in the nonpolar environment: the migration of the solvent anion, though fast, has an activation energy many times higher than that of ordinary ions in supercritical CO_2.[15]

There are also several examples of high mobility solvent *holes* (in cycloalkanes) for which the charge hopping is both fast and has low activation barrier.[56] For these, the case was made that the positive charge is shared by several solvent molecules, it is this sharing that decreases the barrier for the migration.[56] Once more, the high mobility species is a multimer ion.

Given these examples and the arguments considered above, it likely that the high mobility anion-1 is a multimer anion in which the charge is spread over several acetonitrile molecules. Due to the reduction in the charge on the individual molecules, their bending is less strenuous and the barrier for the migration of the multimer anion is low. Such a multimer anion is no different from the "solvated electron" in alkanes (see below), which accounts for the striking similarity between the absorption spectra of anion-1 and "solvated/trapped electrons" in saturated hydrocarbons. *We suggest that acetonitrile provides a rare example of a liquid in which the "solvated electron", multimer anion, coexists with a molecular, dimer, radical anion.*

5.3. Multimer Anion. Assume that anion-1 is a multimer anion of acetonitrile. What is the likely structure of such an anion? The only way to answer this question is to consider a sufficiently large $\{CH_3CN\}_n^-$ cluster. As mentioned in section 2, in the gas phase, only large cluster anions ($n > 12$) are stable. Thus, the model cluster should also be large, too large for a first-principle calculation. On the other hand, if the cluster is too small, the multimer anion with a core other than the dimer anion would be unstable.

To investigate a possible structure of the multimer anion, we modeled a $\{CH_3CN\}_3^-$ cluster using a density functional (B3LYP)[43] method in Gaussian 98.[57] A 6-31+G** basis set that included polarized *(d,f)* and diffuse functions has been used (like in ref 13b). C_{3h} symmetry was imposed and the geometry optimized. In some calculations, a "ghost" hydrogen atom with zero charge was placed at the center of the cluster (Figure 7) to provide s-functions for the "solvated electron"; this "ghost" atom turned out to be unnecessary. Figure 7(b) shows the optimum structure for the $\{CH_3CN\}_3^-$ cluster in a vacuum, Figure 7(a) shows the same for a "solvated" cluster. To obtain the latter, we used polarizable (overlapping spheres) continuum model of Tomasi et al.[44] implemented in the integral equation formalism (IEF PCM). In the latter calculation, the free energy of solvation was ∼−1.05 eV. In both calculations, the lowest energy state was a "propeller-like" $^2A'$ state. The CCN angle in the acetonitrile subunits is 178° in a vacuum and 168° in solution (vs 180° in the neutral molecule). This bending is considerably smaller than in the monomer and dimer anions shown in Figures 2S and 3S. The solvated cluster is more compact: the closest methyl hydrogens (H_{10}) is 1.705 Å away from the symmetry center vs 2.53 Å in a vacuum. The C−C bond in the acetonitrile subunits is elongated from 1.44 Å[28] to 1.475 Å (in solution) or 1.47 Å (in a vacuum), whereas the C−N bond is changed very slightly (1.13 Å[28] to 1.138 Å). In the following, we consider the electronic structure of the "solvated" cluster anion in more detail.

Figures 8 and 22S show the SOMO density in the "solvated" cluster. It is immediately seen that the SOMO envelopes the whole cluster. The main negative nodes are on methyl carbons, while the main positive nodes are at the center, on the in-plane hydrogens, and on carbonyl carbons. This structure may be viewed both as a multimer anion and a "solvated electron", that is, the 1s electron centered at the "solvation cavity": the SOMO has a noticeable s-character at the center (∼0.34), though the main spin density is on the methyl carbons. The latter atoms exhibit large hyperfine coupling constants (hfcc) for ^{13}C: the isotropic hfcc is 6.9 mT; the anisotropy is negligible. Isotropic hfcc for methyl protons are relatively small: 0.19 mT for in-plain hydrogens (the principal values of the dipole tensor are −0.29, −0.15, and 0.44 mT) and −0.086 mT for out-of-plain hydrogens (−0.29, −0.16, and +0.45 mT, respectively). The isotropic hfcc for cyanide ^{13}C and ^{14}N nuclei are 0.4 mT and 0.36 mT, respectively.

The structure bears strong resemblance to the "trapped electron" in saturated hydrocarbons considered by Kevan and co-workers.[4,7,58,59] The "electron" is "solvated" by methyl groups; the positive charge on these groups is increased due to considerable elongation of C−C bonds. This elongation, as demonstrated by our calculations, is the consequence of large electron density on the skeletal carbon atoms. In the semicontinuum model of Kevan and co-workers[4,7] this (multielectron) interaction is treated in terms of a "polarizable" C−C

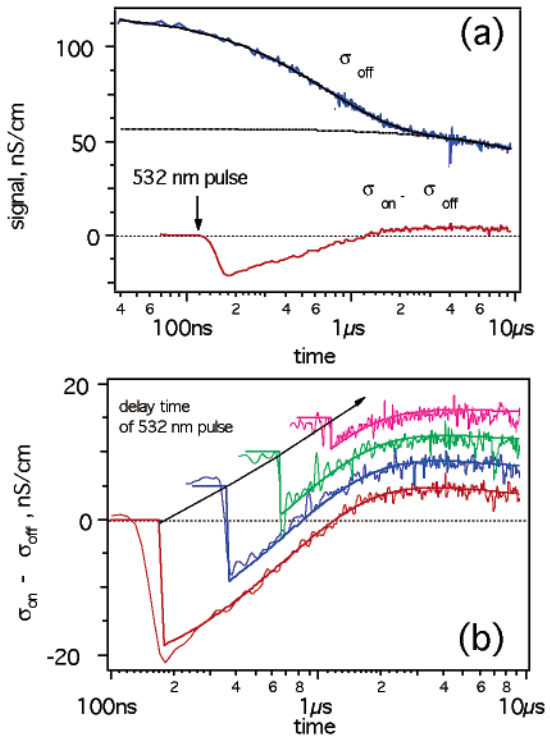

Figure 5. (a) Typical conductivity, σ_{off}, and photobleaching recovery, $\sigma_{on} - \sigma_{off}$, kinetics observed upon 532 nm laser excitation (8.6 ns fwhm, $J_p = 0.3$ J/cm^2) of 300 μM benzene solution in argon-saturated acetonitrile (23C, 2 cm cell, 1.23 kV/cm). The solution was photoionized at $t = 0$ using a 248 nm pulse; the 532 nm laser pulse is delayed by 173 ns relative to this 248 nm pulse. Trace σ_{off} is obtained without 532 nm photoexcitation; solid and dotted lines drawn through the data points have the same meaning as in Figure 1. Trace $\sigma_{on} - \sigma_{off}$ is obtained by numerical subtraction of the decay kinetics obtained with (σ_{on}) and without (σ_{off}) the 532 nm pulse. Immediately after the 532 nm pulse, the conductivity decreases due to fragmentation of anion-2 (in rapid equilibrium with high-mobility anion-1); the decay kinetics of the $\sigma_{on} - \sigma_{off}$ and σ_{off} traces are similar. The small positive persistent signal after 1 μs is due to higher mobility of CN^- relative to impurity anion. (b) Photobleaching recovery kinetics as a function of the delay time of the 532 nm laser pulse. For clarity, these kinetics were vertically spaced. The delay times are 173, 385, 685, and 1200 ns (from bottom to top). Solid lines drawn through the points are the least-squares fits obtained using eqs 3 and 8 for $\Phi = 0.514$ and $\mu_c/\mu_b = 1.22$. The same parameters were used for all four traces; see section 4.2A for more detail.

bond; our calculation justifies their *ad hoc* approach. The size of the solvation cage, the juxtaposition of methyl groups, and the hfcc tensors for methyl protons compare favorably with those obtained experimentally by Kevan and co-workers for the "trapped electron" in frozen 3-methylpentane.[58] Therefore, we expect that the multimer $\{CH_3CN\}_n^-$ anion absorbs much like the "solvated/trapped electron" in alkanes.[2,8,42] Interestingly, our calculation predicts large spin densities for ^{13}C nuclei in the methyl groups that line the "trap" walls; as far as we know, these hyperfine coupling constants have not been determined experimentally. The measurement of these constants would be the ultimate test for our *ab initio* model as well as the semicontinuum model of Kevan and co-workers.[4,7]

Although a first-principle calculation for a larger cluster is impractical, it is possible to make an educated guess as to what happens to the anion when the cluster size increases. The "propeller" structure obtained for the $\{CH_3CN\}_3^-$ anion is similar (save for the elongated C−C bonds) to that of the $\{CH_3CN\}_n X^-$ (X = I, Br) cluster for $n = 3$.[60] One may expect that this trend will pertain to larger size clusters. When the halide

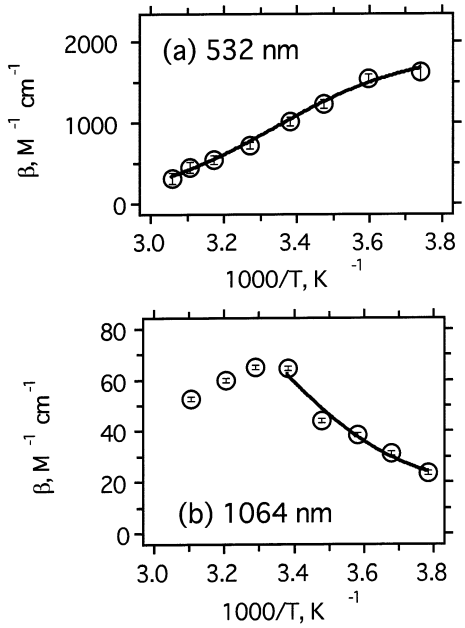

Figure 6. Temperature dependencies in Ar-saturated acetonitrile of the initial slopes $\beta = \partial\Phi/\partial J_p$ for (a) 532 nm and (b) 1064 nm photoexcitation of the solvent anions. These slopes were obtained by exponential fits of the photon fluence dependencies shown in Figures 15S and 16S. The solid lines are the least-squares fits obtained using eqs (12), (13), and (15). See sections 4.2A,B for more detail.

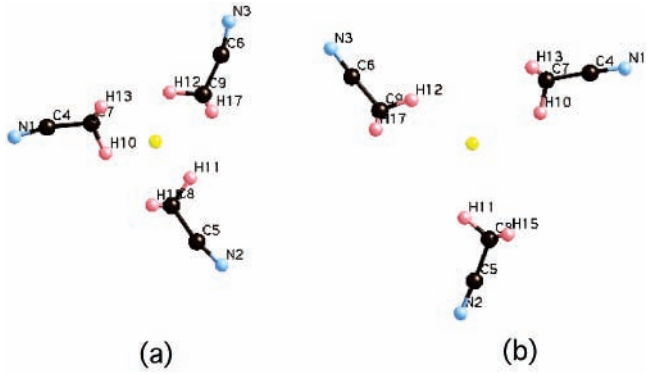

Figure 7. Optimized geometry for the ground $^2A'$ state of C_{3h} symmetric trimer radical anion, $\{CH_3CN\}_3^-$, obtained using B3LYP/6-31+G** calculation (a) using the polarizable continuum solvation model of Tomasi et al. (ref 44) and (b) in a vacuum. Both structures are drawn to the same scale. In the presence of the acetonitrile solvent, the trimer is more compact, and there is a significant spin density on the central "ghost" atom (see the text). A PDF color version of this figure is in the Supporting Information.

Figure 8. Map of the SOMO for the trimer radical anion shown in Figure 7(a). *From left to right:* ±0.03, ±0.02, and ±0.01 density surfaces. Positive lobes are in gray (red), negative lobes an in black (blue). A PDF color version of this figure is in the Supporting Information.

anion is solvated by less than seven acetonitrile molecules, the core anion is a "star" structure with radial CH_3CN dipoles looking away from the halide anion.[60] For $n > 9-12$, the molecules in the first solvation shell couple in an antiparallel

fashion to the molecules in the second solvation shell, so that some molecules in the first solvation shell are oriented tangentially rather than radially.[60] We speculate that relatively small ($n < 6$) solvated $\{CH_3CN\}_n^-$ clusters are also star-shaped. Due to the further spread of the electron density in such clusters, the 1s-character of the SOMO increases, whereas the CCN bending and C−C bond elongation decreases: such an anion would be more like a "solvated electron".

6. Conclusion

The following scenario of electron localization in liquid acetonitrile is suggested: There are two solvent anions, a stable dimer radical anion (anion-2) that absorbs in the visible and a metastable multimer radical anion (anion-1) that absorbs in the IR. The dimer anion has the same structure as the radical anion observed in irradiated α-acetonitrile, with a C−C bond between cyanide carbons.[24] Metastable anion-1 is 0.46 eV more energetic and has abnormally high mobility, due to rapid charge hopping. The electronic structure of this multimer anion is similar to that of "trapped electrons" in glassy alkanes.[4,7] This species is unstable toward dimerization of the molecules in the first and second solvation shells. The two solvent anions are in a rapid dynamic equilibrium. At 25 °C, the settling time of this equilibrium is ∼3 ns. Both of these anions are involved in charge-transfer reactions with electron acceptors. In addition, anion-2 exhibits an unusual proton-transfer reaction with aliphatic alcohols that involves a hydrogen-bonded solute dimer as the proton donor (section 2S).

The suggestion by Bell, Rogers, and Burrows[19] that anion-1 is a monomer radical anion of CH_3CN is not supported by our data. Even in dilute hydrocarbon solution, electron attachment to acetonitrile does not yield CH_3CN^-. Instead, a "solvated electron" that is dipole-bound to the CH_3CN molecule is formed. This species readily loses the negative charge back to the solvent bulk, both by thermal and photo- excitation (sections 4.1 and 1S).

Note Added in Proof. After this article had been submitted in the final form, we became aware of a study by Xia, Peon, and Kohler (kohler@chemistry.ohio-state.edu) on femtosecond electron ejection in liquid acetonitrile (submitted to *J. Chem. Phys.*). These authors demonstrated the formation of NIR-absorbing anion-1 in <300 fs after photoionization of iodide and indole, and concluded that it is a solvated electron. Their kinetic measurement yields a rate constant of $\sim 10^{11}$ M^{-1} s^{-1} for a charge transfer reaction of anion-1 (well before the equilibrium onset), in good agreement with the estimate given in section 4.2C. However, their estimate for the setting time of anion equilibrium at 25 °C (∼260 ps) is substantially lower than ours (∼3 ns).

Acknowledgment. We thank Prof. F. Williams for many useful discussions and Drs. C. D. Jonah and S. Chemerisov for operation of the linac. I.A.S. thanks Dr. V. F. Tarasov for his help with EPR experiments. This work was performed under the auspices of the Office of Science, Division of Chemical Science, US-DOE under Contract No. W-31-109-ENG-38.

Supporting Information Available: (1) Electron attachment to CH_3CN in *n*-hexane; (2) proton-transfer reactions of anion-2 with water and alcohols; (3) solute−solvent interactions in acetonitrile solutions; (4) photoionization of aromatic dopants in frozen alkyl nitriles; (5) additional references; (6) captions to Figures 1S to 26S; (7) a PDF file containing Figures 1S to 26S; (8) a PDF file containing color versions of Figures 1 to 8. This material is available free of charge via the Internet at http://pubs.acs.org.

References and Notes

(1) *Excess Electrons in Dielectric Media*; Ferradini, C., Jay-Gerin, J.-P., Eds.; CRC Press: Ann Arbor, 1991.

(2) Pikaev, A. K. *The Solvated Electron in Radiation Chemistry*; Israel Program for Scientific Translations: Jerusalem, 1971.

(3) Jortner, J. **1959**, *30*, 839; Springlet, B. E.; Jortner, J.; Cohen, M. H. *J. Chem. Phys.* **1968**, *48*, 2720; Jortner, J.; Gaaton, A. *Can. J. Chem.* **1977**, *55*, 1801; Jortner, J. *Ber. Bunsen-Ges. Phys. Chem.* **1971**, *75*, 696.

(4) Kevan, L. *J. Phys. Chem.* **1978**, *82*, 1144.

(5) Rips, I. *J. Chem. Phys.* **1997**, *106*, 2702; Rips, I. *Chem. Phys. Lett.* **1995**, *245*, 79; Rips, I.; Klafter, J.; Jortner, J. *J. Chem. Phys.* **1988**, *89*, 4288.

(6) Brodsky, A. M.; Tsarevsky, A. V. *Adv. Chem. Phys.* **1980**, *44*, 483; Brodsky, A. M.; Tsarevsky, A. V. *J. Phys. Chem.* **1984**, *88*, 3790; Brodsky, A. M.; Vannikov, A. V.; Chubakova, T. A.; Tsarevsky, A. V. *J. Chem. Soc., Faraday Trans. 2* **1981**, *77*, 709.

(7) Kimura, T.; Fueki, K.; Narayana, P. A.; Kevan, L. *Can. J. Chem.* **1977**, *55*, 1940; Feng, D.-F.; Kevan, L.; Yoshida, H. *J. Chem. Phys.* **1974**, *61*, 4440; Nishida, M. *J. Chem. Phys.* **197**, *65*, 5242.

(8) Ichikawa, T.; Yoshida, H. *J. Chem. Phys.* **1980**, *73*, 1540.

(9) Sheu, W.-S.; Rossky, P. J. *Chem. Phys. Lett.* **1993**, *202*, 186; Sheu, W.-S.; Rossky, P. J. *Chem. Phys. Lett.* **1993**, *213*, 233; Sheu, W.-S.; Rossky, P. J. *J. Am. Chem. Soc.* **1993**, *115*, 7729.

(10) Borgis, D.; Staib, A. *J. Chim. Phys.* **1996**, *93*, 1628; Borgis, D.; Staib, A. *J. Chem. Phys.* **1996**, *104*, 9027; Borgis, D.; Staib, A. *J. Chem. Phys.* **1995**, *103*, 2642; Borgis, D.; Staib, A. *J. Phys. Condens. Matter* **1996**, *8*, 9389; Borgis, D.; Staib, A. *Chem. Phys. Lett.* **1994**, *230*, 405.

(11) Schnitker, J.; Rossky, P. J.; Kenney-Wallace, G. A. *J. Chem. Phys.* **1986**, *85*, 2986; Motakabbir, K. A.; Rossky, P. J. *Chem. Phys.* **1989**, *129*, 253; Motakabbir, K. A.; Schnitker, J.; Rossky, P. J. *J. Chem. Phys.* **1992**, *97*, 2055.

(12) Barnett, R. N.; Landman, U.; Nitzan, A. *J. Chem. Phys.* **1990**, *93*, 8187; Barnett, R. N.; Landman, U.; Nitzan, A. *J. Chem. Phys.* **1989**, *90*, 4413.

(13) (a) Tauber, M. J.; Mathies, R. A. *J. Phys. Chem. A* **2001**, *105*, 10 952; Mizuno, M.; Tahara, T. *J. Phys. Chem. A* **2001**, *105*, 8823; (b) Kim, K. S.; Park, I.; Lee, S.; Cho, K.; Lee, J. Y.; Kim, J.; Joannopoulos, J. D. *Phys. Rev. Lett.* **1996**, *76*, 956; Turi, L. *J. Chem. Phys.* **1999**, *110*, 10 364; Novakovskaya, Y. V.; Stepanov, N. F. *Chem. Phys. Lett.* **2001**, *344*, 619, and references therein.

(14) (a) van den Ende, C. A. M.; Nyikos, L.; Sowada, U.; Warman, J. M.; Hummel, A. *J. Electrostatics* **1982**, *12*, 97; van den Ende, C. A. M.; Nyikos, L.; Sowada, U.; Warman, J. M.; Hummel, A. *Radiat. Phys. Chem.* **1982**, *19*, 297; van den Ende, C. A. M.; Nyikos, L.; Sowada, U.; Warman, J. M.; Hummel, A. *J. Phys. Chem.* **1980**, *84*, 1155 (b) Itoh, K.; Holroyd, R. *J. Phys. Chem.* **1990**, *94*, 8850.

(15) Shkrob, I. A.; Sauer, M. C., Jr. *J. Chem. Phys. B* **2001**, *105*, 4520.

(16) Shkrob, I. A.; Sauer, M. C., Jr. *J. Chem. Phys. B* **2001**, *105*, 7027.

(17) Desfrançois, C.; Abdoul-Carmie, H.; Adjouri, C.; Khelifa, N.; Schermann, J. P. *Europhys. Lett.* **1994**, *26*, 25; Bailey, C. G.; Dessent, C. E. H.; Johnson, M. A.; Bowen, K. H., Jr. *J. Chem. Phys.* **1996**, *104*, 6976.

(18) Singh, A.; Gesser, H. D.; Scott, A. R. *Chem. Phys. Lett.* **1968**, *2*, 271.

(19) Bell, I. P.; Rodgers, M. A. J.; Burrows, H. D. *J. Chem. Soc.* **1976**, 315.

(20) Williams F.; Sprague, E. D. *Acc. Chem. Res.* **1982**, *15*, 408.

(21) Bonin, M. A.; Lin, J.; Tsuji, K.; Williams, F. In *Radiation Chemistry − II, Advances in Chemsitry Series*, Vol. 82; American Chemical Society: Washington, DC, 1968; pp 269−290.

(22) Sprague, E. D. Ph.D. Thesis, University of Tennessee, June 1971; pp 115−117.

(23) Mulac, W. A.; Bromberg, A.; Meisel, D. *Radiat. Phys. Chem.* **1985**, *26*, 205.

(24) Shkrob, I. A.; Takeda, K.; Williams, F. *J. Phys. Chem. A* **2002**, *106*, 9132.

(25) Renner, T. A.; Blander, M. *J. Phys. Chem.* **1977**, *81*, 857.

(26) Siebers, J. G.; Buck, U.; Beu, T. A. *Chem. Phys.* **1998**, *129*, 549.

(27) Mitsuke, K.; Kondow, T.; Kuchitsu, K. *J. Phys. Chem.* **1986**, *90*, 1505.

(28) Barrow, M. J. *Acta Crystallogr. B* **1981**, *37*, 2239.

(29) Torrie, B. H.; Powell, B. M. *Mol. Phys.* **1992**, *75*, 613.

(30) Hirata, Y.; Mataga, N.; Sakata, Y.; Misumi, S. *J. Phys. Chem.* **1983**, *87*, 7, 1493; Hirata, Y.; Mataga, N.; Sakata, Y.; Misumi, S. *J. Phys. Chem.* **1982**, *86*, 1508; Hirata, Y.; Mataga, N. *J. Phys. Chem.* **1983**, *87*, 1680.

(31) Chandra, H.; Symons, M. C. R. *J. Chem. Soc., Faraday Trans. 1* **1988**, *84*, 3401.

(32) Taub, I. A.; Harter, D. A.; Sauer, M. C., Jr.; Dorfman, L. M. *J. Chem. Phys.* **1964**, *41*, 979; Jha, K. N.; Freeman, G. R. *J. Chem. Phys.* **1968**, *48*, 5480; Arai, S.; Kira, A.; Imamura, M. *J. Phys. Chem.* **1970**, *74*, 2120; Fletcher, J. W.; Richards, P. J.; Seddon, W. A. *Can. J. Chem.* **1970**, *48*, 1645; Rzad, S. J.; Fendler, J. H. *J. Chem. Phys.* **1970**, *52*, 5395; Seki, H.; Imamura, M. *Bull. Chem. Soc. Jpn.* **1971**, *44*, 1538.

(33) Shida, T.; Imamura, M. *J. Phys. Chem.* **1974**, *78*, 233; Kenney-Wallace, G. A.; Hall, G. E.; Hunt Billard, L. A.; Sarantidis, K. *J. Phys. Chem.* **1980**, *84*, 1145; Billard, L. A. H.; James, F. C.; Kenney-Wallace, G. A. *J. Phys. Chem.* **1983**, *87*, 2981; C. Silva, P. K. Walhout, P. J. Reid, P. F. Barbara, *J. Phys. Chem. A* **1998**, *102*, 5701.

(34) Badger, B.; Brocklehurst, B. *Trans. Faraday Soc.* **1969**, *65*, 2582; Miller, J. H.; Andrews, L.; Lund, P. A.; Schatz, P. N. *J. Chem. Phys.* **1980**, *73*, 4932; Mehnert, R. In *Radical Ionic Systems*; Kluwer: Amsterdam, 1991; p 231; Mehnert, R.; Brede, O. *Radiat. Phys. Chem.* **1985**, *26*, 353; Mehnert, R.; Brede, O.; Naumann, W. *Ber. Bunsen-Ges. Phys. Chem.* **1984**, *88*, 71.

(35) Michel, H.; Lippert, E. In *Organic Liquids*; Buckingham, A. D., Lippert, E., Bratos, S., Eds.; Wiley: New York, 1978; p 293; see also p 13.

(36) (a) Whittenburg, S. L.; Wang, C. H. *J. Chem. Phys.* **1977**, *66*, 4255. (b) Knozinger, K.; Leutloff, D.; Wittenbeck, R. *J. Mol. Struct.* **1980**, *60*, 115; (c) Kovacs, H.; Kowalewski, J.; Maliniak, A.; Stilbs, P. *J. Phys. Chem.* **1989**, *93*, 962. (d) Strizhakova, N. G.; Shevchenko, Yu. B.; Trachevski, V. V.; Kozachkov, S. G.; Maletin, Yu. A. *Ukr. Chem. J.* **1997**, *63*, 26. (e) Kratochwill, V. A.; Weidner, J. U.; Zimmermann, H. *Ber. Bunsen-Ges. Phys. Chem.* **1973**, *77*, 408.

(37) Stokes, R. H. *J. Chem. Soc., Faraday Trans. 1* **1977**, *73*, 1140; Smith, F.; Brown, I. *Aust. J. Chem.* **1973**, *26*, 691;

(38) Baxendale, J. H.; Rasburn, E. J. *J. Chem. Soc., Faraday Trans. 1* **1974**, *70*, 705; Baxendale, J. H.; Sharpe, P. H. G. *Chem. Phys. Lett.* **1976**, *41*, 440; Gangwer, T. E.; Allen, A. O.; Holroyd, R. A. *J. Phys. Chem.* **1977**, *81*, 1469; Kenney-Wallace, G. A.; Jonah, C. D. *J. Phys. Chem.* **1982**, *86*, 2572.

(39) Safonova, L. P.; Patsatsiya, B. K.; Kolker, A. M. *Russ. J. Phys. Chem.* **1992**, *66*, 2201; Safonova, L. P.; Patsatsiya, B. K.; Kolker, A. M. *Russ. J. Phys. Chem.* **1994**, *68*, 37.

(40) Nogami, T.; Mizuhara, T.; Kobayashi, N.; Aoki, M.; Akashi, T.; Shirota, Y.; Mikawa, H.; Sumitani, M. *Bull. Chem. Soc. Jpn.* **1981**, *54*, 1559; Taniguchi, Y.; Nishina, Y.; Mataga, N. *Bull. Chem. Soc. Jpn.* **1972**, *45*, 2923.

(41) Vauthey, E.; Haselbach, E.; Suppan, P. *Helv. Acta* **1987**, *70*, 347; Delcourt, M. O.; Rossi, M. J. *J. Phys. Chem.* **1982**, *86*, 3233.

(42) See, for example, Gillis, H. A.; Klassen, N. V.; Teather, G. C.; Lokan, K. H. *Chem. Phys. Lett.* **1971**, *10*, 481; Gillis, H. A.; Klassen, N. V.; Woods, R. J. *Can. J. Chem.* **1977**, *55*, 2022; Wang, H. Y.; Willard, J. E. *J. Chem. Phys.* **1978**, *69*, 2964.

(43) Becke, A. D. *Phys. Rev. A* **1988**, *38*, 3098; Lee, C.; Yang, W.; Parr, R. G. *Phys. Rev. B* **1988**, *37*, 785.

(44) Tomasi, J.; Persico, M. *Chem. Rev.* **1994**, *94*, 2027; Cancès, E.; Mennucci, B.; Tomasi, J. *J. Chem. Phys.* **1997**, *107*, 3032.

(45) Itoh, K.; Holroyd, R. *J. Phys. Chem.* **1990**, *94*, 8854.

(46) Holroyd, R. A. *Ber. Bunsen-Ges. Phys. Chem.* **1977**, *81*, 298.

(47) Sowada, U.; Holroyd, R. A. *J. Chem. Phys.* **1979**, *70*, 3586; Lukin, L. V.; Yakovlev, B. S. *Chem. Phys. Lett.* **1976**, *42*, 307.

(48) Holroyd, R. A.; Gangwer, T. E.; Allen, A. O. *Chem. Phys. Lett.* **1975**, *31*, 520; Lukin, L. V.; Yakovlev, B. S. *High Energy Chem.* **1977**, *11*, 440.

(49) Chen, P.; Holroyd, R. A. *J. Phys. Chem.* **1996**, *100*, 4491.

(50) Lukin, L. V.; Yakovlev, B. S. *Int. J. Radiat. Chem.* **1975**, *7*, 667.

(51) When two alcohol molecules form a dimer in a nonpolar solution, an enlargement of one of the dipole moments occurs [see: Bordewijk, P.; Kunst, M.; Rip, A. *J. Phys. Chem.* **1973**, *77*, 548; Campbell, C.; Brink, G.; Glasser, L. *J. Phys. Chem.* **1975**, *79*, 661]. For example, for heptanol-1 in CCl_4, the dipole moment of the monomer and dimer species are 1.66 and 3.53 D, respectively; for octanol-1 in CCl_4 − 1.64 and 3.41 D, respectively.

(52) von Raumer, M.; Suppan, P.; Jacques, P. *J. Photochem. Photobiol. A* **1997**, *105*, 21.

(53) Jackowski, K. *Chem. Phys. Lett.* **1992**, *194*, 167 and references therein.

(54) Fletcher, W. H.; Shoup, C. S. *J. Mol. Struct.* **1963**, *10*, 300.

(55) Bowen, K. H.; Eaton, J. G. In *The Structure of Small Molecules and Ions*; Naamna, R., Vagar, Z., Eds.; Plenum: New York, 1987; p 147; DeLuca, M. J.; Niu, B.; Johnson, M. *J. Chem. Phys.* **1988**, *88*, 5857; Tsukuda, T.; Johnson, M.; Nagata, T. *Chem. Phys. Lett.* **1997**, *268*, 429; Zhou, M.; Andrews, L. *J. Chem. Phys.* **1999**, *110*, 2414 and 6820; Thompson, W. E.; Jacox, M. E. *J. Chem. Phys.* **1999**, *111*, 4487; and Thompson, W. E.; Jacox, M. E. *J. Chem. Phys.* **1989**, *91*, 1410.

(56) Warman, J. M. In *The Study of Fast Processes and Transient Species by Electron-Pulse Radiolysis*; Baxendale, J. H., Busi, F., Eds.; Reidel: Dordrecht, The Netherlands, 1982; p 433; Shkrob, I. A.; Sauer, M. C., Jr.; Trifunac, A. D. In *Radiation Chemistry: Present Status and Future Prospects*; Jonah, C. D., Rao, B. S. M., Eds.; Elsevier: Amsterdam, 2001; p 175; Shkrob, I. A.; Sauer, M. C., Jr.; Trifunac, A. D. *J. Phys. Chem. B* **2000**, *104*, 3752 and 3760.

(57) Frisch, M. J.; Trucks, G. W.; Schlegel, H. B.; Scuseria, G. E.; Robb, M. A.; Cheeseman, J. R.; Zakrzewski, V. G.; Montgomery, J. A., Jr.; Stratmann, R. E.; Burant, J. C.; Dapprich, S.; Millam, J. M.; Daniels, A. D.; Kudin, K. N.; Strain, M. C.; Farkas, O.; Tomasi, J.; Barone, V.; Cossi, M.; Cammi, R.; Mennucci, B.; Pomelli, C.; Adamo, C.; Clifford, S.; Ochterski, J.; Petersson, G. A.; Ayala, P. Y.; Cui, Q.; Morokuma, K.; Malick, D. K.; Rabuck, A. D.; Raghavachari, K.; Foresman, J. B.; Cioslowski, J.; Ortiz, J. V.; Stefanov, B. B.; Liu, G.; Liashenko, A.; Piskorz, P.; Komaromi, I.; Gomperts, R.; Martin, R. L.; Fox, D. J.; Keith, T.; Al-Laham, M. A.; Peng, C. Y.; Nanayakkara, A.; Gonzalez, C.; Challacombe, M.; Gill, P. M. W.; Johnson, B. G.; Chen, W.; Wong, M. W.; Andres, J. L.; Head-Gordon, M.; Replogle, E. S.; Pople, J. A. *Gaussian 98*, revision A.1; Gaussian, Inc.: Pittsburgh, PA, 1998.

(58) Kevan, L.; Ichikawa, T. *J. Phys. Chem.* **1980**, *84*, 3260.

(59) Noda, S.; Kevan, L.; Fueki, K. *J. Phys. Chem.* **1975**, *79*, 2866.

(60) Markovich, G.; Perera, L.; Berkowitz, M. L.; Cheshnovsky, O. *J. Chem. Phys.* **1996**, *105*, 2675; Ayala, R.; Martinez, J. M.; Pappalardo, R. R.; Marcos, E. S. *J. Phys. Chem. A* **2000**, *104*, 2799.